Stable anticipation synchronization in mutually coupled vertical-cavity surface-emitting lasers system

Ning Jiang (江 宁), Wei Pan (潘 炜), Bin Luo (罗 斌), Weili Zhang (张伟利), and Di Zheng (郑 狄)

Center of Information Photonics and Communications, Southwest Jiaotong University, Chengdu 610031

Two vertical-cavity surface-emitting lasers (VCSELs) are mutually coupled through a partially transparent mirror (PTM) placed in the pathway. The PTM plays the role of external mirror, which controls the feedback strength and coupling strength. We numerically simulate this system by establishing a visible SIMULINK model. The results demonstrate that the anticipation synchronization is achieved and it can tolerate some extent frequency detuning. Moreover, the system shows similar chaos-pass filtering effect on unidirectionally coupled system even both VCSELs are modulated. This system allows simultaneously bidirectional secure message transmission on public channels.

OCIS codes: 060.4370, 140.1540, 140.3570, 140.5960.

doi: 10.3788/COL20080607.0517.

A semiconductor laser with external perturbation, such as external optical feedback[1], optical injecting[2,3] etc., shows chaotic behaviors, and the chaotic signals can be used to encrypt small–amplitude message onto or into it with appropriate encryption schemes such as chaos masking (CMA)[4], chaos shift keying (CSK)[5], or chaos modulation (CMO)[6]. The experiment in Athens[7] confirmed the potential of this technique. While most of the schemes considered only unidirectional coupling, the chaotic output of the transmitter is unidirectionally injecting into the receiver, and two types of synchronization, which are named complete synchronization (CS) and general synchronization (GS)[6,8], exist in the systems.

Mutually coupled VCSELs showing complex nonlinear behaviors and synchronization performance were proved by Li and Zhang *et al.*[3,9]; on the other hand, Klein *et al.*[10] showed that it might be possible to use the synchronization of two symmetry chaotic semiconductor lasers for novel cryptographic key-exchange protocols, by which the secret messages could be transmitted over public channels without using any previous secrets. However, there is a well-known problem that the stable synchronization condition of mutually coupled system is too strict to apply practically, because there is some difference between the transmitter and the receiver, more or less. A tiny frequency detuning would destroy the synchronization, or cause a leader/laggard configuration.

In this letter, a partially transparency mirror (PTM)[11] is placed between two vertical-cavity surface emitting lasers (VCSELs) as shown in Fig. 1. The two facets of PTM play the roles of external mirrors. We ignore the loss when light propagates through the PTM, and the relation between the transmission and reflectivity coefficients is $T_i + R_i = 1$. The output of one VCSEL is partially reflected back to itself as external feedback light by the PTM; the residual light propagates through the PTM, and couples to the other VCSEL. The total light injected to the VCSELs is the sum of the delay self-feedback light from PTM and the light coming from the opposite VCSEL. L is the distance between the two VCSELs, which determines the flight time between the two VCSELs; L_i is the distance between the VCSELi and PTM, which determines the feedback delay time of VCSELi. The sum of feedback strength k_i and coupling strength σ_{3-i} to the other VCSEL is K_i, which is dependent on the facet reflectivity of VCSELi.

In general, to numerically model a VCSEL, it is necessary to consider its multi-transverse mode characteristic and its polarization characteristic etc. in the rate equations. But in the chaos synchronization system, we mainly concentrate on dynamical behaviors of lasers outputs, a simplified model named Lang-Kobayashi equations[1−6,8−15] based on the mean-field theory (MFT) has been proved to be sufficient to describe the dynamics of outputs of semiconductor lasers and show no effect on the encryption/decryption performance of the system. The dynamic behaviors of VCSEL1 are given by the coupled differential equations for photons number density P, the time dependent on optical phase Φ, and the carrier density N, as

$$\frac{\mathrm{d}P_1(t)}{\mathrm{d}t} = (\Gamma_L \Gamma_z G_1 - \frac{1}{\tau_p})P_1(t) + 2\frac{k_1}{\tau_{in}}\sqrt{P_1(t)P_1(t-\tau_{f1})}\cos[\omega_1\tau_{f1} + \Phi_1(t) - \Phi_1(t-\tau_{f1})]$$

$$+2\frac{\sigma_1}{\tau_{in}}\sqrt{P_1(t)P_2(t-\tau_{21})}\cos[\omega_2\tau_{21} + \Phi_1(t) - \Phi_2(t-\tau_{21}) - \Delta\omega t] + \beta_{sp}\beta N_1^2(t), \tag{1}$$

$$\frac{\mathrm{d}\Phi_1(t)}{\mathrm{d}t} = \frac{\beta_c}{2}(\Gamma_L\Gamma_z G_1 - \frac{1}{\tau_p}) - \frac{k_1}{\tau_{in}}\sqrt{P_1(t-\tau_{f1})/P_1(t)}\sin[\omega_1\tau_{f1} + \Phi_1(t) - \Phi_1(t-\tau_{f1})]$$

$$-\frac{\sigma_1}{\tau_{in}}\sqrt{P_2(t-\tau_{21})/P_1(t)}\sin[\omega_2\tau_{21} + \Phi_1(t) - \Phi_2(t-\tau_{21}) - \Delta\omega t], \tag{2}$$

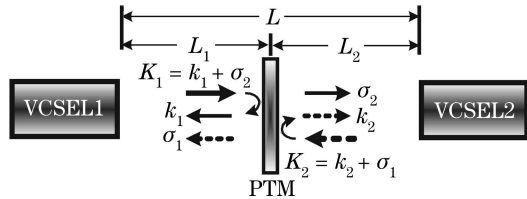© 2008 Chinese Optics Letters

Fig. 1. Schematic of two-VCSEL mutually coupled system.

$$\frac{dN_1(t)}{dt} = \frac{I}{e\pi r^2 d} - \frac{N_1(t)}{\tau_e} - G_1 P_1(t), \qquad (3)$$

where Γ_L and Γ_z are the lateral and longitudinal confinement factors, respectively; τ_p is the photon lifetime; τ_{in} is the laser cavity round-trip time; $\tau_{fi} = 2L_i/c$ is the feedback delay time of VCSELi, where c is the velocity of light; $\tau_{ij} = L/c$ is the flight time between VCSELs; $\Delta\omega = \omega_1 - \omega_2$, ω is the optical frequency; B_{sp} is the bimolecular recombination coefficient; β is the spontaneous emission factor; β_c is the linewidth broadening factor; e is the electron charge; τ_e is the carrier lifetime; d is the thickness of active region; r is the core radius. $\pi r^2 d$ denotes the volume of active region, the small r and d result in small active region volume which is one or two orders of magnitude less than that of edge emitting lasers (EELs), and the small volume makes the pumping much efficient. The micro-cavity effect of VCSEL makes its threshold much lower by improving the spontaneous emission rate. To better characterize the special quantum well's active layer, we choose the logarithm form of optical gain for the two VCSELs[1,3,10]:

$$G_1 = v_g \alpha_N \lg[N_1(t)/N_0]/(1 + \varepsilon_{NL} |P_1(t)|), \qquad (4)$$

where v_g is the group velocity, α_N is the gain coefficient, ε_{NL} is the gain suppress factor. Likewise for VCSEL2 when indices 1 and 2 are exchanged, the symbol "$-$" before the detuning frequency $\Delta\omega$ is replaced by "$+$".

In our simulations, $L = 1.5$ m, $K_1 = K_2 = 10^{-2}$. The internal parameters are assumed to be identical for the two VCSELs: the operation wavelength $\lambda_0 = 980$ nm, $\Gamma_L = 1$, $\Gamma_z = 0.07$, $\tau_p = 2.47$ ps, $v_g = 8.1 \times 10^9$ cm/s, $\alpha_N = 1392$ cm^{-1}, the transparency carrier density $N_0 = 1.3 \times 10^{18}$ cm^{-3}, $\tau_{in} = 0.15$ ps, $\beta_c = 4.8$, $\tau_e = 2.7$ ns, $\beta = 10^{-4}$, $\beta_{sp} = 1 \times 10^{-10}$ cm^{6}s^{-1}, $\varepsilon_{NL} = 1 \times 10^{-17}$ cm^3, $d = 1 \times 10^{-5}$ cm, and $r = 5$ μm[1].

Figure 2 shows the shift correlation coefficient $\rho(\Delta t)$[8,13,15], which is obtained by calculating the correlation coefficient between the outputs of the two VCSELs when output of VCSEL1 is continuously shifted in time with respect to that of VCSEL2. The six graphs exhibit the dynamics of synchronization for different locations of the PTM, where the reflection and transmission coefficients are both equal to 50% of K; the system satisfied the delay-time condition (DTC) DTC1 in Ref. [12], which requires $k_1 = \sigma_1 = k_2 = \sigma_2$ and $\tau_{f1} + \tau_{f2} = \tau_{12} + \tau_{21}$ to get identical sum of feedback and injecting light.

In all graphs there is a max[ρ_{max}] of $\rho(\Delta t)$ for each location, which denotes high quality synchronization between the two VCSELs, and we find that the lag time between the two VCSELs is $\Delta t = \tau_{f2} - \tau_{12} = -\tau_{f1} + \tau_{21}$, this is in line with the results in Refs. [12,13]. The position of PTM determines the lag time and leader/laggar roles, if PTM is closer to VCSEL1, then it leads to VCSEL2, and
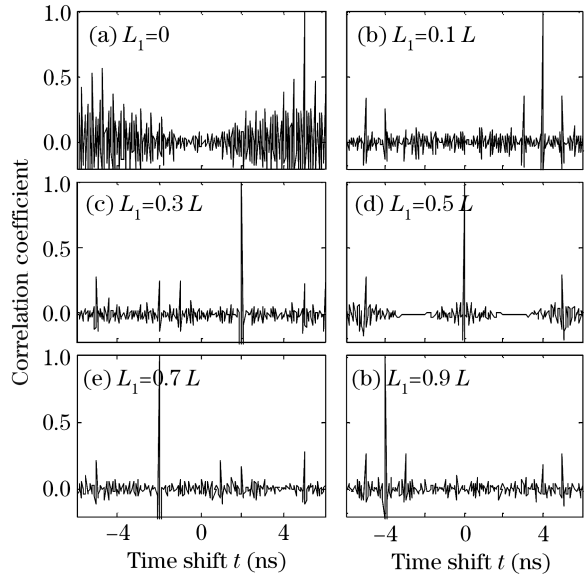

Fig. 2. Isochronal synchronization for different positions of the PTM.

vice versa; when the mirror is moved to the center, ρ_{max} moves toward zero shifts. The peaks at $\pm\tau_{ij}$ represent the effect of the coupling. It is obvious that the feedback is dominated; the small difference of the two peaks is due to the different initial conditions. On the other hand, it is evident that the curves are symmetry at the maximum peaks; this is because the system is symmetry-keeping when the PTM is placed at any location between VCSELs.

When the PTM is fixed at the middle of the two VCSELs, the system satisfied the DTC2 and DTC3 in Ref. [12], which requires that $k_1 = k_2$, $\tau_{f1} = \tau_{f2}$ (or $2\tau_{f1} = 2\tau_{f2} = \tau_{12} + \tau_{21}$), then the lag $[\Delta t = (\tau_{12} - \tau_{21})/2]$ is zero because of the identical flight time. We repeat the simulations by changing the reflectivity and transmission coefficients, and get high quality instantaneous chaos synchronization similar to the results in Ref. [13].

Table 1 shows the maximum correlation coefficients

Table 1. Maximum Correlation Coefficients for Different PTM Locations

Δf (GHz)	$L_1 = 0.1L$	$L_1 = 0.3L$	$L_1 = 0.5L$	$L_1 = 0.7L$	$L_1 = 0.9L$
-4.5	0.7026	0.7408	0.6268	0.6862	0.5826
-3.5	0.7917	0.6861	0.7297	0.6455	0.7455
-2.5	0.8601	0.7820	0.7896	0.7118	0.8057
-1.5	0.9154	0.8533	0.8660	0.8259	0.9044
-1	0.9325	0.9274	0.8923	0.8923	0.9161
-0.5	0.9728	0.9725	0.9555	0.9646	0.9630
0	1	1	1	1	1
0.5	0.9778	0.9716	0.9636	0.9898	0.9691
1	0.9237	0.8964	0.8922	0.9225	0.9168
1.5	0.9133	0.9208	0.8609	0.8953	0.8801
2.5	0.8446	0.8198	0.8140	0.8404	0.7889
3.5	0.7540	0.7756	0.7421	0.7626	0.7737
4.5	0.6977	0.7742	0.6472	0.5782	0.6750

ρ_{max} versus the detuning frequency for different PTM locations. It is evident that this system can tolerate some extent frequency detuning for any PTM location (Δf from -1.5 to 1.5 GHz), the tolerance of frequency detuning at all locations are similar, and these results are similar to those in Ref. [14]. It is worth mentioning that the lag time between the VCSELs is still $\Delta t = \tau_{\mathrm{f2}} - \tau_{12} = -\tau_{\mathrm{f1}} + \tau_{21}$. This kind of lag time is different from that occurring in mutually coupled systems without self-feedback light, in which the lag time is the injecting time[2]. This is because that the two VCSELs receive the same feedback signal even if their history is different. It is then easier for them to remain synchronized because the difference in their delayed values does not affect the synchronization[15]. This phenomenon can also be explained by calculating the distribution of Lyapunov Exponents.

Finally, to investigate the encryption and decryption characters of this system, we study the chaos-pass filtering (CPF) effect with an additional small-amplitude sinusoidal signal modulating the VCSELs. Figure 3(a) shows the CPF effect of this system with VCSEL1 modulated by small signal while VCSEL2 not. The modulation frequency is 2 GHz, and the amplitude is 5% of injecting DC current I. Obviously, in spectrum of VCSEL1 (top curve), there is a peak at the modulation frequency (marked with arrow), but this does not occur in spectrum of VCSEL2 (bottom curve). It indicates that the CPF effect is obvious, so the encrypted messages transmitted from VCSEL1 can be decoded from VCSEL2. This phenomenon is similar to that of unidirectionally coupled system. In Fig. 3(b), both VCSELs are modulated, where VCSEL1 is similar in Fig. 3(a), VCSEL2 is modulated by a sinusoidal signal with 1-GHz frequency and $0.05I$ amplitude. Similar to the phenomenon in Fig. 3(a), both VCSELs spectra show good CPF effects at the modulation frequency. It is worth noticing that the spectra of VCSEL1 are different in some extent this is because in the mutually-coupled systems, the lasers are highly sensitive to the variation of its opposite. The additional modulation of VCSEL2 changes the output of VCSEL2, and then the light injected to VCSEL1 is changed, so its spectrum is affected. We repeated the simulations by

change modulation index of VCSEL2 from 0.05 to 0.005 gradually. The results indicate that even the modulation index of VCSEL2 is very small, its affection on the spectrum of VCSEL1 is still obvious. Although the spectra of VCSEL1 are different in the two case, the high quality synchronization is not changed, which is verified by comparing the peaks of the VCSELs' spectra in Fig. 3. This kind of mutually-affecting CPF effect can be named mutual chaos pass filtering (MCPF) effect, it provides two advantages: it allows message transmission on public channels; it allows for simultaneously bidirectional communication. With MCPF procedure, the listener on the public channels between the VCSELs can just decrypt the message difference $m_1(t) - m_2(t + \Delta t)$ at best, only the transmitter VCSEL1 can decrypt the correct message from VCSEL2 by subtract $m_1(t) - m_2(t + \Delta t)$ from $m_1(t)$, and likewise for VCSEL2.

In conclusion, we have investigated a system consists of two VCSELs, with a PTM between them, the numerical results show that the anticipation synchronization is achieved, and the lag time between the two VCSELs is just determined by feedback delay time, independent of the flight time even the frequency detuning is considered. Moreover, the investigations of chaos pass filtering effect show that our results strengthen the suitability of such a synchronization scheme for simultaneously bidirectional secure optical communication on public channels.
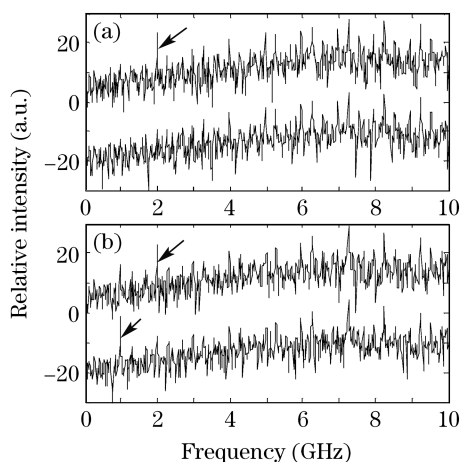
Fig. 3. Chaos pass filtering effect of the system. (a) VCSEL1 modulated and VCSEL2 unmodulated; (b) both VCSELs modulated. The top curve is spectrum of VCSEL1, and the bottom curve is spectrum of VCSEL2.

References

1. S. F. Yu, IEEE J. Quantum Electron. **35,** 332 (1999).
2. W. Zhang, W. Pan, B. Luo, X. Li, X. Zou, and M. Wang, Chinese J. Lasers (in Chinese) **34,** 53 (2007).
3. X. Li, W. Pan, B. Luo, D. Ma, Z. Zhao, and G. Deng, Chin. Opt. Lett. **2,** 278 (2004).
4. S. Yan, Chin. Opt. Lett. **3,** 283 (2005).
5. C. R. Mirasso, J. Mulet, and C. Masoller, IEEE Photon. Technol. Lett. **14,** 456 (2002).
6. X. Li, W. Pan, B. Luo, and D. Ma, IEEE J. Quantum Electron. **42,** 953 (2006).
7. A. Argyris, D. Syvridis, L. Larger, V. Annovazzi-Lodi, P. Colet, I. Fisher, J. Garcia-Ojalvo, C. R. Mirassl, L. Pesquera, and K. A. Shore, Nature **437,** 343 (2005).
8. X. Li, W. Pan, D. Ma, B. Luo, W. Zhang, and Y. Xiong, Acta Phys. Sin. (in Chinese) **55,** 5094 (2006).
9. W. Zhang, W. Pan, B. Luo, X. Zou, M. Wang, and Z. Zhou, Opt. Lett. **33,** 237 (2008).
10. E. Klein, N. Gross, E. Kopelowitz, M. Rosenbluh, L. Khaykovich, W. Kinzel, and I. Kanter, Phys. Rev. E **74,** 046201 (2006).
11. R. Vicente, C. R. Mirasso, and I. Fischer, Opt. Lett. **32,** 403 (2007).
12. M. C. Chiang, H.-F. Chen, and J.-M. Liu, Opt. Commun. **261,** 86 (2006).
13. M. C. Chiang, H.-F. Chen, and J.-M. Liu, IEEE J. Quantum Electron. **41,** 1333 (2005).
14. N. Gross, W. Kinzel, I. Kanter, M. Rosenbluh, and L. Khaykovich, Opt. Commun. **267,** 464 (2006).
15. E. Klein, N. Gross, M. Rosenbluh, W. Kinzel, L. Khaykovich, and I. Kanter, Phys. Rev. E **73,** 066214 (2006).